

# Freezing Stochastic Travelling Waves

G. J. Lord\*

V. Thümmeler†

DRAFT April 20, 2011

## Abstract

The aim of this paper is to investigate new numerical methods to compute travelling wave solutions and new ways to estimate characteristic properties such as wave speed for stochastically forced partial differential equations. As a particular example we consider the Nagumo equation with multiplicative noise which we mainly consider in the Stratonovich sense. A standard approach to determine the position and hence speed of a wave is to compute the evolution of a level set. We compare this approach against an alternative where the wave position is found by minimizing the  $L^2$  norm against a fixed profile. This approach can also be used to stop (or freeze) the wave and obtain a stochastic partial differential algebraic equation that we then discretize and solve. Although attractive as it leads to a smaller domain size it can be numerically unstable due to large convection terms. We compare numerically the different approaches for estimating the wave speed. Minimization against a fixed profile works well provided the support of the reference function is not too narrow. We then use these techniques to investigate the effect of both Itô and Stratonovich noise on the Nagumo equation as correlation length and noise intensity increases.

## 1 Introduction

The effects of stochastic forcing on solutions of stochastic partial differential equations (SPDEs) have recently received a great deal of attention in applications ranging from material science, atmosphere modelling to neural science. Of particular interest are the effects of noise on travelling waves and fronts as these are often physically important solutions. We use the term travelling wave to include fronts and waves and develop in this paper numerical methods to solve for stochastic versions of these objects.

We consider the stochastic PDE

$$du = \left[ u_{xx} + f(u) \right] dt + g(u, t) \circ dW(t), \quad \text{given } u(0) = u^0, \quad x \in \mathbb{R}. \quad (1)$$

Although the noise term is written here as a Stratonovich integral we consider below the noise in both a Stratonovich and Itô sense. For ease of exposition we take  $u : \mathbb{R} \times \mathbb{R}_+ \rightarrow \mathbb{R}$  although similar numerical procedures have been applied to systems of PDEs and waves in  $\mathbb{R}^2$ , see for example [5]. For additive noise the function  $g$  is taken as a constant whereas for multiplicative noise  $g$  depends on  $u$ . In the case of no noise ( $g = 0$ ) we recover the deterministic PDE

$$u_t = u_{xx} + f(u), \quad \text{given } u(0) = u^0, \quad x \in \mathbb{R}. \quad (2)$$

In the deterministic case the analysis of travelling waves both analytically and by numerics is a mature field. This is not the case for SPDEs where much of the analysis is performed for specific equations or for the case of small noise. Indeed with stochastic forcing existence for all time of these waves is not guaranteed and the definition of quantities such as wave speed vary from system

---

\*Department of Mathematics and Maxwell Institute, Heriot-Watt University, Edinburgh, EH4 1ER, UK, [g.j.lord@hw.ac.uk](mailto:g.j.lord@hw.ac.uk)

†Universität Bielefeld, Bielefeld, Germany, [thuemmle@math.uni-bielefeld.de](mailto:thuemmle@math.uni-bielefeld.de)

to system. Typically the position of a stochastic travelling wave is determined from the position of a level set. For small noise the centres of these fronts can be shown to follow a rescaled Brownian motion, see [34, 8, 14]. In the case of multiplicative noise the front may exist for all times and the wave front may have compact support [36] and is well-defined over some time varying interval in space  $[a(t), b(t)]$  and takes stationary values out side of this interval. There is a well developed literature for the stochastic Fisher–Kolmogorov–Piscounov equation [12, 11, 26, 39] with waves defined in this form. Multiplicative noise is seen to change the wave speed of the wave and the position is seen to diffuse from the mean (or Goldstein mode), for reviews see [16, 27]. However, it is not our aim to replicate these results here. We investigate different ways to measure the wave speed, using the level set approach as well as a new approach of minimizing the  $L^2$  norm of the wave against a fixed profile. Furthermore we apply different computational techniques to compute time dependent waves - this includes freezing the wave to stop it from travelling. We extend a numerical method introduced in [6] for deterministic PDEs of the form (2). This method freezes the wave in the computational domain by adding a convection term to the equation to compensate for the movement of the wave. The convection term that gives the speed of the wave is determined from an extra algebraic condition from the  $L^2$  minimization and the wave speed is explicitly solved for as a time dependent quantity. Convergence of this method for PDEs was considered in [37] and stability of the wave considered in [38]. We use these techniques to obtain new computational results on the effect of multiplicative noise on the wave speed of the Nagumo equation with Stratonovich and Itô noise. In contrast to [16, 3, 2], we present new numerical results on the effect of spatial correlation length on the width of the wave and compare different measures of the wave speed. These results include our new idea of comparing the wave to a reference function. Furthermore we present new results for Itô and additive noise.

Numerically we solve for the wave profile and a time dependent wave speed for (1) which is, in the case of stochastic forcing, a random variable. As a specific example to illustrate the computational method and to compare against existing techniques we consider the scalar Nagumo equation [18]

$$du = [u_{xx} + u(1-u)(u-\alpha)] dt + (\nu + \mu u(1-u)) \circ dW. \quad (3)$$

With  $\nu \neq 0$  and  $\mu = 0$  we have additive noise and  $\mu \neq 0$  the noise is multiplicative. For multiplicative noise we have that  $u = 0$  and  $u = 1$  are stationary and numerical simulations suggest a wave exists between them [3, 2]. The deterministic equation

$$u_t = u_{xx} + u(1-u)(u-\alpha), \quad u(x, t) \in \mathbb{R}, \quad x \in \mathbb{R}, \quad t > 0, \quad (4)$$

is often used for testing algorithms since travelling wave solutions  $u(x, t) = u_{\text{det}}(x - ct)$  connecting the stationary points  $u_- = 0$ ,  $u_+ = 1$  of this equation are explicitly known besides other explicit solutions, such as pulses, sources and sinks [1, 9]. These travelling wave solutions depend on the nonlinearity and the leading profile of initial data  $u^0$ . Define the function  $u_k(x)$  by

$$u_k(x) = (1 + e^{-kx})^{-1}. \quad (5)$$

We use this function to specify both initial data  $u^0$  and reference functions that have different profiles (by varying  $k$ ). For  $\alpha \in (0, 1/2]$  there is a unique asymptotic travelling wave where as for  $\alpha \in (-1, 0]$  the asymptotic profile and the wave speed depends on the leading profile  $e^{k_0 x}$  of the initial data as  $x \rightarrow \infty$ . We summarize results below for the deterministic Nagumo equation, these are found, for example, in [16].

- For  $\alpha \in (0, 1/2]$  the solution  $u = u_k$ , with  $k = 1/\sqrt{2}$  is asymptotically stable and all initial front data  $u^0$  is attracted to this wave. The asymptotic wave speed is given by  $c = -\sqrt{2} (\frac{1}{2} - \alpha)$ .
- For  $\alpha \in (-1/2, 0]$  if the initial data  $u^0 = u_{k_0}$  has  $k_0 \geq k_* = -\alpha\sqrt{2}$  then the asymptotic speed is given by  $c = -\sqrt{2} (\frac{1}{2} - \alpha)$ . If  $k_0 < k_*$  then the asymptotic wave speed is  $\geq (k_0^2 - \alpha)/k_0$ .
- For  $\alpha \in (-1, -1/2]$  if the initial data  $u^0 = u_{k_0}$  is such that  $k_0 \geq k_{\dagger} = \sqrt{|\alpha|}$  then the asymptotic speed is given by  $2k_{\dagger}$ . If  $k_0 < k_{\dagger}$  then the asymptotic speed is  $\geq 2k_{\dagger}$ .

The outline of the rest of the paper is as follows. We review in Section 2 the computation of travelling waves in the deterministic case and extend to the case of stochastic forcing. We discuss measures of wave speeds of a stochastic travelling wave and discuss the numerical approximation. In Section 3 we illustrate the numerical method on the Nagumo equation with multiplicative noise. We compare solving the stochastic partial differential equation (SPDE) and the stochastic partial differential algebraic equation (SPDAE) where the wave is frozen by minimizing the  $L^2$  distance between a reference function and the travelling wave. We compare the different measures of wave speeds. We illustrate from numerics that although a feasible method it can lead to numerical instability. We investigate the effect of the choice of reference function  $\hat{u}$  in Section 3.2.2. In Section 3.3 we present new numerical results for Itô and Stratonovich multiplicative noise on how the wave speed changes with noise intensity. We also present new results on the effect of the spatial correlation length. Additive noise is considered in Section 3.5 where we again examine the wave speed with noise intensity and illustrate the SPDAE approach when new travelling waves are nucleated. Finally we consider weaker versions of the stochastic travelling wave fixed in the computational domain by mean wave speeds and then discuss the results and computational method.

## 2 Stochastic travelling waves

In this section we introduce the (stochastic) differential algebraic equations that we use to define the travelling wave problem. We start by reviewing the more familiar deterministic case before considering the case with stochastic forcing. In both cases we reduce the infinite problem to finite dimensions by truncating the computational domain and discretizing in space.

### 2.1 Deterministic PDE and discretization

Let us assume that equation (2) has a travelling wave solution  $u$ , so that  $u$  can be written as

$$u(x, t) = u_{\text{det}}(\xi), \quad \xi = x - \lambda_{\text{det}}t, \quad (6)$$

where  $u_{\text{det}} \in \mathcal{C}_b^2(\mathbb{R}, \mathbb{R}^m)$  denotes the waveform and  $\lambda_{\text{det}}$  its wave speed. In a comoving frame  $v(\xi, t) = u(\xi - \lambda_{\text{det}}t, t)$  equation (2) reads

$$v_t = v_{\xi\xi} + \lambda_{\text{det}}v_{\xi} + f(v), \quad \xi \in \mathbb{R}, \quad t \geq 0 \quad (7)$$

of which the travelling wave  $u_{\text{det}}$  is a stationary solution. Since the wave speed  $\lambda_{\text{det}}$  is generally unknown we transform equation (2) into a co-moving frame with unknown position  $\gamma(t)$ , i.e. we insert the ansatz  $v(x, t) = u(x - \gamma(t), t)$  into (2). Then we obtain

$$v_t = v_{xx} + \lambda v_x + f(v), \quad (8)$$

where  $\lambda(t) = \gamma'(t)$ . In order to compensate for the additional variable  $\lambda$  we add a so called phase condition

$$0 = \psi(v, \lambda) \quad (9)$$

which together with (8) forms a partial differential algebraic equation (PDAE) [6]. The position  $\gamma$  of the wave can then be calculated by integrating  $\gamma' = \lambda, \gamma(0) = 0$  to get

$$\gamma(t) = \int_0^t \lambda(s) ds. \quad (10)$$

For the numerical implementation we need to truncate the spatial domain from  $x \in \mathbb{R}$  to  $x \in [0, L]$  and impose appropriate boundary conditions such as Neumann, Dirichlet or projection boundary conditions [37]. We then solve (8) and (9) for  $x \in [0, L]$ . In contrast to traditional deterministic travelling wave computations where the steady states of (7) are solved for with appropriate boundary conditions this method does not rely on  $\lambda$  being a constant wave speed.

Thus far we have not discussed the choice of the phase fixing function  $\psi$  in (9). Since the phase condition only selects one representative out of the infinite family of solutions, there is some freedom of choice here. The simplest phase condition is to align the solution with respect to a given reference function  $\hat{u}$ . It is natural to take the  $L^2$  norm since we then the minimum can be found by differentiation and equating to zero (see eg [7]). For two functions  $v$  and  $w$  to minimize over shifts in space  $y$  the  $L^2$  norm:  $\min_y \|v(x, \cdot) - w(x - y, \cdot)\|_2$ . Differentiating and equating to zero we find that

$$\int (v(x, \cdot) - w(x - y, \cdot)) w_x dx = 0.$$

So for the PDE we take the phase condition to be :

$$\psi_{\text{fix}}(u) = \langle \hat{u}_x, u - \hat{u} \rangle.$$

This choice was termed the template fitting method in [32].

In our numerical simulations we will discretize in space using standard uniformly spaced finite differences, so we discretize on a finite grid  $x_0, \dots, x_M$ ,  $u(x_j) = u_j$ . For the second derivative with  $M$  points and spatial step  $\Delta x$  we approximate the derivative  $\partial_{xx} \approx A$  where  $A = \frac{1}{\Delta x^2} B \in \mathbb{R}^{M-2, M-2}$  for Dirichlet boundary conditions and for Neumann boundary conditions,

$$A = \frac{1}{\Delta x^2} \begin{pmatrix} -2 & 2 \\ & B \\ & 2 & -2 \end{pmatrix} \in \mathbb{R}^{M, M}, \quad \text{with} \quad B = \begin{pmatrix} -2 & 1 & & \\ 1 & \ddots & \ddots & \\ & \ddots & \ddots & 1 \\ & & 1 & -2 \end{pmatrix}.$$

We choose not to use periodic boundary conditions since we compute a travelling front rather than a pulse and this would require a domain of twice the size and also introduces two travelling waves that travel in opposite directions. Neumann and Dirichlet boundary conditions were shown to work well in the deterministic case in [37, 38]. For the first spatial derivative we introduce  $(D_R u)_j = (u_{j+1} - u_j)/\Delta x$ ,  $(D_L u)_j = (u_j - u_{j-1})/\Delta x$ ,  $(D_C u)_j = (u_{j+1} - u_{j-1})/(2\Delta x)$  for  $j = 1, \dots, M-1$  using Dirichlet boundary conditions  $u^0 = \gamma_L, u_M = \gamma_R$  or Neumann boundary conditions  $u^0 = u_1, u_{M-1} = u_M$ . For convection terms we either use  $D_C$  or, where up-winding is an issue, we choose the appropriate  $D_L, D_R$  or a weighted combination [6]

$$\partial_x \approx D_h := e^{-\beta\mu} D_L + (1 - e^{-\beta h}) D_R, \quad (11)$$

where  $\beta$  is a parameter ( $\beta = 0$  or  $\beta = \frac{1}{2}$  in our computations) and in what follows  $h$  will be some function of the wave speed. Recent work by Hairer and Voss [17] examine the discretization of the advection term  $uu_x$  for the stochastic Burger's equation and show that the limit is dependent on the discretization. The form of advection for the Burger's equation and considered here is different and as we can compare to cases without the advection term we did not note and discretization dependent

Discretizing in space with  $N$  grid points and after eliminating the boundary conditions we obtain the following DAE system for  $\lambda \in \mathbb{R}$  and  $v \in \mathbb{R}^{N-2}$  for Dirichlet or  $v \in \mathbb{R}^N$  for Neumann boundary conditions

$$\begin{aligned} v' &= Av + \lambda(D_\lambda v + \eta) + f(v) + \varphi \\ 0 &= \langle \hat{u}_x, v - \hat{u} \rangle, \end{aligned} \quad (12)$$

where the vectors  $\varphi, \eta$  are used to deal with the boundary conditions. This system can be solved by using appropriate DAE solvers [4] or we can use a linear implicit Euler method to obtain the fully discrete system

$$\begin{aligned} v^{n+1} &= v^n + \Delta t [Av^{n+1} + \lambda^{n+1}(D_{\lambda^n} v^n + \eta) + f(v^n) + \varphi] \\ 0 &= \langle D_C \hat{u}, v^{n+1} - \hat{u} \rangle \end{aligned} \quad (13)$$

which leads to

$$\begin{pmatrix} I - \Delta t A & -\Delta t(D_{\lambda^n} v^n + \eta) \\ \Delta x D_C \hat{u}^T & 0 \end{pmatrix} \begin{pmatrix} v^{n+1} \\ \lambda^{n+1} \end{pmatrix} = \begin{pmatrix} v^n + \Delta t(f(v^n) + \varphi) \\ \langle D_C \hat{u}, \hat{u} \rangle \end{pmatrix}.$$

Note that for the reference or template  $\hat{u}_x$  we use the central difference approximation  $D_C$  since this is most accurate and convection instabilities are not an issue for this term.

Under a uniqueness assumption of the travelling wave of the PDE it was shown in [37] that for  $L \rightarrow \infty$  and  $\Delta x \rightarrow 0$  the stationary solution of (12) converges to the exact travelling wave solution. Moreover the solution of (12) inherits the nonlinear stability properties of (2). Numerically we observe below that the DAE system correctly computes the travelling wave depending even when the travelling wave is not unique, see Section 3.

## 2.2 Stochastic PDE and stochastic travelling wave

We seek travelling wave solutions to the Stratonovich SPDE

$$du = [u_{xx} + f(u)] dt + g(u) \circ dW, \quad u(0) = u^0 \quad (14)$$

or the ItôSPDE

$$du = [u_{xx} + f(u)] dt + g(u) dW, \quad u(0) = u^0 \quad (15)$$

with  $g(u) = \nu + \mu h(u)$ , where  $\nu$  and  $\mu$  are parameters that allow us to consider additive and multiplicative noise. Results on the existence of a solution for (14) and (15) with  $x \in \mathbb{R}$  domain can be found in [40]. For the stochastic Allen-Cahn equation with spatially smooth, bounded additive noise existence is shown in [31]. A recent paper [43] shows existence for the non-Lipschitz cases for space time white noise.

We truncate the infinite domain and consider (14) (or (15)) on a large finite domain so that  $x \in [0, L]$  with either Neumann or Dirichlet boundary conditions. For the finite domain with  $x \in [0, L]$  we refer to [10, Theorem 7.4] with  $f$  and  $g$  satisfying global Lipschitz conditions, [28] for some weaker conditions and recent results in [19] for non-Lipschitz  $g$ . For the stochastic Nagumo equation we have  $f(u) = u(1-u)(u-\alpha)$  and take  $h(u) = u(1-u)$ .

We consider noise  $W(t)$  to be a  $Q$ -Wiener process [10], and assume that covariance operator  $Q$  and the linear operator  $\partial_{xx}$  have the same eigenfunctions  $\phi_j$ . If the covariance operator has eigenvalues  $\zeta_j \geq 0$  then we can write

$$W(x, t) = \sum_{j \in \mathbb{Z}} \zeta_j^{1/2} \phi_j(x) \beta_j(t), \quad (16)$$

for independent Brownian motions  $\beta_j$ . We take space-time noise that is white in time with exponential decay in the spatial correlation length  $\xi > 0$  in which case

$$\mathbb{E}(dW(x, t)dW(y, s)) = C(x-y)\delta(t, s), \quad C(x) = \frac{1}{2\xi} \exp\left(-\frac{\pi x^2}{4\xi^2}\right).$$

We approximate using (16) by taking  $\zeta_n = \exp(-\frac{\xi^2 \lambda_j}{L})$ , where  $\lambda_j = \frac{j^2 \pi^2}{L^2}$  and  $L$  is the length of the interval [35, 21].

In the Stratonovich case (14) we can eliminate the systematic effects of the noise on the drift and convert to an Itô integral. This gives an additional term to the nonlinearity so that the Stratonovich SPDE (14) is equivalent to the Itô SPDE

$$du = [u_{xx} + \tilde{f}(u)] dt + g(u) dW \quad (17)$$

where  $\tilde{f}(u) = f(u) - C(0)g'(u)g(u)$ , see for example [16]. We can also convert from the Itô interpretation (15) to a Stratonovich by

$$du = [u_{xx} + \tilde{f}(u)] dt + g(u) \circ dW \quad (18)$$

where now  $\tilde{f}(u) = f(u) + C(0)g'(u)g(u)$ .

We discretize the SPDE in space by finite differences and evaluate the noise on the spatial grid. In time we discretize with a constant time step  $\Delta t$ . For the noise term we have an increment

$$\Delta W_n = \sum_{j \in [-J, J]} \zeta_j^{1/2} \phi_j(x) \xi_j,$$

where  $\xi_j \sim N(0, \Delta t)$ . To compute directly with the Stratonovich noise for (14) we use the standard Heun method [15, 20] and also the semi-implicit Euler–Heun method

$$\begin{aligned} z &= u^n + g(u^n) \Delta W_n \\ u^{n+1} &= u^n + \Delta t [A u^{n+1} + f(u^n) + \varphi] + \frac{1}{2} (g(z) + g(u^n)) \Delta W_n \end{aligned} \quad (19)$$

where  $\Delta W_n$  is an increment of the noise and  $\varphi$  arises from the boundary conditions.

Although intuitively it is understood what is meant by a stochastic travelling wave it is not easy to find a definition in the literature, however for a review see [16, 27]. Typically a stochastic travelling wave and speed is either defined by the evolution of a level set such as in [26, 39] or through the evolution relative to a deterministic wave, such as through a small noise expansion such as in [23]. We will apply our methods to the case where in the deterministic case the travelling wave is known to be unique and also where it is not unique.

Consider the SPDE with a well defined wave with compact support as defined in [36], so that at  $u(-\infty, \cdot) = u_-$ ,  $u(\infty, \cdot) = u_+$ . We can then define a travelling wave and wave speed using the points

$$a(t) := \sup\{z : u(x, t) = u_-, x \leq z\}, \quad b(t) := \sup\{z : u(x, t) = u_+, x \geq z\}, \quad (20)$$

and in addition we can take the 'mid point' level set of a wave

$$c(t) := \sup\{z : u(x, t) = (u_- + u_+)/2, x \leq z\}. \quad (21)$$

These level sets define the position of the travelling wave. Note that we take the supremum as there may be multiple crossings through the level set (see for example Figure 5) for the front. Given the positions an 'instantaneous' wave speed can be determined from the  $a$ ,  $b$  and  $c$  by differentiation. We report below a wave speed  $\Lambda_z(t)$ ,  $z \in \{a, b, c\}$  defined by

$$\Lambda_z(t) = \mathbb{E} \left( \frac{z(t) - z(t_0)}{t - t_0} \right) \quad z \in \{a, b, c\} \quad (22)$$

where the expectation is taken over the number of realizations. We may choose the initial time  $t_0$  to either be at the start of the computation  $t_0 = 0$  or some later time ( $t_0 > 0$ ) to avoid transient effects. We believe This differs from the definition of wave speed used in computations by [3, 2, 24] where they report  $z(t)/t$  for  $z \in \{a, b, c\}$ . Numerically, these level set points  $a, b, c$  are found by evolving the SPDE (14) directly and interpolating over the grid.

If we assume the wave has some long time invariant speed an alternative definition of the wave speed is to fit a linear polynomial  $P_{\Lambda_{\text{fit}}}$  to the data  $(t, \mathbb{E}z(t))$ ,  $z \in a, b, c$ ,  $t \geq t_0$  where

$$P_{\Lambda_{\text{fit}}}(t) := \Lambda_{\text{fit}} t + K \quad (23)$$

Wave speeds may then be estimated by  $\Lambda_{\text{fit}z}$ ,  $z \in a, b, c$  where we may take  $t_0 > 0$  to avoid transients. Although this is a trivial extension of wave speed defined by (22) we have not seen it reported in the literature.

Finally we introduce a novel measure of the wave speed for SPDEs through minimization of the  $L^2$  norm  $\|u(x, t) - \hat{u}(x - y, t)\|^2$  against a fixed profile  $\hat{u}$ . This is similar to the freezing the wave in the deterministic case. We solve the SPDE and compute the position  $\gamma(t)$  of the wave. We then move the reference function relative to the travelling wave solution  $u$ . That is we solve SPDE

$$du = [u_{xx} + f(u)] dt + g(u) \circ dW, \quad u(0) = u^0$$

and couple this to a reference function  $\hat{u}(x, t)$  that moves so that

$$\langle \hat{u}_x(t), u(t) - \hat{u}(t) \rangle = 0. \quad (24)$$

Numerically this requires interpolation onto the spatial grid at each time step. We compute an instantaneous wave speed  $\lambda(t)$  and this is related to the position of the wave through  $\gamma(t) = \int_0^t \lambda(s) ds$ . A wave speed  $\Lambda_{\min}$  is then defined through the time average of the instantaneous wave speed  $\lambda$

$$\Lambda_{\min}(t) = \frac{1}{t - t_0} \int_{t_0}^t \mathbb{E}(\lambda(s)) ds. \quad (25)$$

So far we have not commented on the choice of profile  $\hat{u}$  to minimize against.

If a deterministic travelling wave profile exists then this is a natural choice for  $\hat{u}$ . In examples where we do not have an analytic expression for the deterministic travelling wave  $\hat{u}$  then this can be solved for simultaneously or a sample solution solved for and saved. However, this is a matter of choice and we could minimize the  $L^2$  norm against any fixed profile. One obvious choice of profile  $\hat{u}$  is to take the initial data, so that  $\hat{u} = u(0)$ . Note that the choice of  $\hat{u}$  is important. In particular we illustrate in Section 3.2.2 that for a given  $\hat{u}$  the minimization may not be unique and may fail numerically if  $\hat{u}$  has small support.

We again note that from the position data  $(t, \mathbb{E}\gamma(t))$  we can fit a linear polynomial

$$P_{\Lambda_\gamma}(t) := \Lambda_\gamma t + K \quad (26)$$

to obtain an alternative estimate of the average wave speed.

### 2.2.1 Freezing the stochastic travelling wave

Inspired by the deterministic fixing of a wave we freeze a stochastic travelling wave relative to a reference function  $\hat{u}$ , this allows direct computation of the wave speed from the  $L^2$  minimization. We take  $\hat{u}$  to be a fixed continuous function and we evaluate it numerically at the grid points. We examine the Stratonovich SPDE in a co-moving frame as we did for the deterministic case. First let us examine the effects of a shift in space on the covariance of the noise noting that

$$\mathbb{E}(dW(x + r(t), t), dW(y + r(s), s)) = C(x + r(t) - y - r(s))\delta(t - s).$$

We see that for noise that is white in time the covariance is the same in the two frames.

Let's consider the Stratonovich SPDE transforming to the moving frame  $u(x, t) = v(x + \gamma(t), t)$  we have

$$dv(x + \gamma(t), t) = v_x \circ d\gamma(t) + dv$$

and so formally we can write

$$dv = \left[ v_{xx} + \frac{d\gamma(t)}{dt} v_x + f(v) \right] dt + g(v) \circ dW, \quad v(0) = u^0.$$

We introduce the phase condition to determine  $d\gamma$  and minimize the  $L^2$  norm, i.e.  $\langle \hat{u}_x, v - \hat{u} \rangle = 0$ . If we define the random variable  $\lambda$  so that  $\gamma(t) = \int_0^t \lambda(s) ds$  then we seek to solve the SPDAE

$$\begin{aligned} dv &= [v_{xx} + \lambda v_x + f(v)] dt + g(v) \circ dW, \quad v(0) = u^0 \\ 0 &= \langle \hat{u}_x, v - \hat{u} \rangle \end{aligned} \quad (27)$$

In order to compute directly with the Stratonovich noise for (14) we use either the standard Heun method [15, 20] or the semi-implicit Euler–Heun method

$$\begin{aligned} z &= u^n + g(u^n) \Delta W_n \\ u^{n+1} &= u^n + \Delta t [A u^{n+1} + \lambda^n (D_{\lambda^n} u^n + \eta) + f(u^n) + \varphi] + \frac{1}{2} (g(z) + g(u^n)) \Delta W_n \\ 0 &= \langle \hat{u}_x, u^{n+1} - \hat{u} \rangle. \end{aligned} \quad (28)$$

The algorithm yields an approximation  $u^n$ ,  $n = 0, 1, 2, \dots$  to  $u(n\Delta t)$  and  $\lambda^n$ , and approximation to  $\lambda(s)$ . This gives us a numerical scheme for the SPDAE in which the stochastic travelling wave is frozen.

We have a time-dependent random variable  $\lambda(t)$  that we call the instantaneous wave speed. Of more physical interest is the time average of this quantity  $\Lambda_{\min}^{fix}$  that we call the wave speed and report

$$\Lambda_{\min}^{fix} = \frac{1}{t - t_0} \int_{t_0}^t \mathbb{E}\lambda(s) ds. \quad (29)$$

The instantaneous wave speed  $\lambda$  gives the position  $\gamma(t)$  of the wave. If we assume the wave has some long time invariant speed this can be estimated from  $\gamma(t)$  by fitting a linear polynomial

$$P_{\Lambda_{\gamma}^{fix}}(t) := \Lambda_{\gamma}^{fix} t + K \quad (30)$$

to the data from freezing the wave  $(t, \mathbb{E}\gamma(t))$ , for  $t > t_0 \geq 0$ .

The literature on solving stochastic DAEs is in its infancy, however there are some analytic and computational results mainly arising from examining noise in circuit simulations, see for example [33, 30, 41, 42]. We are not aware of work on the existence directly for SPDAE.

Computing a travelling wave through (27) or we introduce the random variable  $\lambda$  which is used to freeze the wave. We could however define a weaker versions by taking statistics of  $\lambda$ . For example we can take the time-averaged wave speed  $\Lambda(t)$  for each realization

$$\begin{aligned} dv &= [v_{xx} + \Lambda_{\min} v_x + f(v)] dt + g(v) \circ dW, \quad v(0) = u^0 \\ 0 &= \psi(v, \lambda). \end{aligned} \quad (31)$$

Other weaker forms of travelling wave solution are possible where the instantaneous wave speed  $\lambda$  or time average wave speed  $\Lambda$  of an individual realization is replaced by its expectation over realizations, for example

$$\begin{aligned} dv &= [v_{xx} + \mathbb{E}(\lambda) v_x + f(v)] dt + g(v) \circ dW, \quad v(0) = u^0 \\ 0 &= \psi(v, \lambda); \end{aligned} \quad (32)$$

and

$$\begin{aligned} dv &= [v_{xx} + \mathbb{E}(\Lambda) v_x + f(v)] dt + g(v) \circ dW, \quad v(0) = u^0 \\ 0 &= \psi(v, \lambda). \end{aligned} \quad (33)$$

Using the sample mean of  $\lambda$  and  $\Lambda$  for fixing we are essentially using a “group velocity” to fix the wave and as a result the mean profile will contain a spread as each individual realization is not fixed at the same point. By taking these weaker notions of wave speed to freeze the wave we observe spreading of the front profiles, as discussed in [16].

### 3 Results for the Nagumo Equation

We compare the different estimates of the wave speed and apply the technique of freezing the wave to the Nagumo equation (3) for both multiplicative and additive space-time white noise. For the majority of our simulations we take  $\Delta x = 0.1$ ,  $\Delta t = 0.05$  and a spatial domain of  $L = 500$  or  $L = 800$  with Neumann boundary conditions and integrate till  $t = 100$ . We compute 100 realizations simultaneously. In our computations of wave speeds unless stated we take  $t_0 = t/2$  to reduce transient effects and we drop the dependence of the computed wave speeds on the time  $t$  and so report  $\Lambda_{\min}$ ,  $\Lambda_{\min}^{fix}$ ,  $\Lambda_{\gamma}$ ,  $\Lambda_z$  and  $\Lambda_{\text{fit } z}$ ,  $z \in \{a, b, c\}$ .

#### 3.1 Deterministic PDE

Before we examine the stochastic PDE we briefly examine deterministic computations. We point out some features of computing the travelling wave and speed by direct simulation of the PDE



$\hat{k} = 1/\sqrt{2}$	Theory	$\Lambda_{\min}$	$\Lambda_a$	$\Lambda_b$	$\Lambda_c$	$\Lambda_{\text{fit}a}$	$\Lambda_{\text{fit}b}$	$\Lambda_{\text{fit}c}$
$k_0 = 1/\sqrt{2}$	1.06066	1.06047	1.06025	1.06027	1.06026	1.06025	1.06026	1.06026
$k_0 = 0.1$	$\geq 2.6$	2.59741	2.59690	2.59689	2.59689	2.59689	2.59689	2.59689

Table 1: Different measures of the wave speed computed from solving the deterministic PDE. To compute  $\Lambda_{\min}$  the profile  $\hat{u}$  travels to minimize the  $L^2$  norm (24). Estimates of wave speeds  $\Lambda_z$ , are from (22) the level set and  $\Lambda_{\text{fit}z}$  from (23) from fitting,  $z \in a, b, c$ . We see these measures of the wave speed agree to 4 decimal places.

$\hat{k} = 1/\sqrt{2}$	Theory	$\Lambda_{\min}^{fix}$	$\Lambda_a$	$\Lambda_b$	$\Lambda_c$	$\Lambda_{\text{fit}a}$	$\Lambda_{\text{fit}b}$	$\Lambda_{\text{fit}c}$
$k_0 = 1/\sqrt{2}$	1.06066	1.06052	2.0e-07	-1.1e-06	1.5e-08	1.8e-07	-9.5e-07	1.4e-08
$k_0 = 0.1$	$\geq 2.6$	2.60048	3.1e-06	-3.6e-07	-1.4e-07	1.3e-06	-8.4e-08	-6.0e-08

Table 2: Wave speeds computed from solving the PDAE and freezing the travelling wave. The fact that the wave does not move in the domain can be seen from the level set wave speeds  $\Lambda_z$  and  $\Lambda_{\text{fit}z}$ ,  $z \in \{a, b, c\}$  which are close to zero. The wave speed  $\Lambda_{\min}^{fix}$  agrees with that computed for the PDE given in Table 1.

(2) versus freezing and solving the PDAE (12). In particular we examine the regime where the travelling wave is not unique and the theory of [37] on freezing the deterministic case no longer holds. For  $\alpha = -0.25$  the asymptotic travelling wave and wave speed depends on the leading profile data of the initial data  $u^0$ . We take two initial profiles  $u^0(x) = u_{k_0}(x)$  with  $k_0 = 0.1 < k_*$  and  $k_0 = 1/\sqrt{2} > k_*$ . To compute the speed by minimization we present results with reference functions  $\hat{u} = u_{\hat{k}}$  with  $\hat{k} = \sqrt{2}$ . Results with a reference function with  $\hat{k} = 0.1$  are identical (see also Section 3.2.2 for comments on the choice of reference function).

We show in Table 1 wave speeds computed from direct simulation of the PDE. For the PDE  $\Lambda_{\min}$  is computed by moving the profile  $\hat{u}$  at the computed wave speed from the minimization using the condition (24). There is good agreement between the computed wave speeds, although  $\Lambda_{\min}$  appears to have converged faster than the other measures of the wave speed to theoretical value. When we freeze the wave in the computational domain and solve the PDAE we see from Table 2 that the wave is frozen (to single precision) since the level set positions of  $a(t), b(t)$  and  $c(t)$  do not change and hence wave speeds  $\Lambda_{\text{fit}z}$ ,  $z \in a, b, c$  from fitting the linear polynomial are zero (to single precision). The wave speed  $\Lambda_{\min}$  estimated from freezing the wave and the minimisation the  $L^2$  norm agrees with the wave speeds computed from the PDE (and is in fact a better approximation to the theoretical values).

### 3.2 Stochastic travelling wave and frozen wave

To illustrate computations for the stochastic PDE we start by taking Stratonovich multiplicative noise with  $\mu = 0.1$  and a correlation length of  $\xi = 0.1$ . In Table 3 we show results from solving the SPDE with the same single realization of the noise using the same two different sets of initial data and two difference reference functions as for the deterministic case. Since we have taken the same noise realization, when initial data is the same our measures of the wave speed  $\Lambda_z$ , and  $\Lambda_{\text{fit}z}$ ,  $z \in a, b, c$  are identical and independent of the reference function  $\hat{u}$ . The choice of reference function does change the wave speed measured by the minimization in approximately the fourth decimal place (compare  $\Lambda_{\min}$  or  $\Lambda_\gamma$  for the different  $\hat{k}$  values in Table 3). This small difference is due to a combination of interpolation errors and is not seen for the SPDAE below where we do not need this interpolation. If we compare the values of the deterministic PDE Table 1 and SPDE case Table 3 for the single realization we see the wave speeds with noise are slightly larger than the deterministic case. In Figure 1 we plot the result of a single realization in (a) for the SPDE with initial data  $u^0$  with  $k_0 = 1/\sqrt{2}$ . The wave front is initially at  $x \approx 200$  and travels to  $x \approx 500$ . For the two different initial data we have plotted in (b) the two distributions of the instantaneous wave

$t_0 = 50, t_1 = 100$	$\Lambda_{\min}$	$\Lambda_\gamma$	$\Lambda_a$	$\Lambda_b$	$\Lambda_c$	$\Lambda_{\text{fit}a}$	$\Lambda_{\text{fit}b}$	$\Lambda_{\text{fit}c}$
$k_0 = 1/\sqrt{2}, \hat{k} = 1/\sqrt{2}$	1.07575	1.06965	1.07484	1.06746	1.07536	1.07149	1.07147	1.06935
$k_0 = 1/\sqrt{2}, \hat{k} = 0.1$	1.07538	1.06987	1.07484	1.06746	1.07536	1.07149	1.07147	1.06935
$k_0 = 0.1, \hat{k} = 0.1$	2.77250	2.78015	2.80594	2.74516	2.76020	2.79657	2.72070	2.78112
$k_0 = 0.1, \hat{k} = 1/\sqrt{2}$	2.77146	2.78178	2.80594	2.74516	2.76020	2.79657	2.72070	2.78112

Table 3: Wave speeds computed from solving a single realization of the SPDE with noise intensity  $\mu = 0.1$  and correlation length  $\xi = 0.1$ . To compute  $\Lambda_{\min}$  the profile  $\hat{u}$  travels with the appropriate speed found by minimization of the  $L^2$  norm.

speed  $\lambda$  used to compute the wave speed through the minimization (with  $\hat{k} = 1/\sqrt{2}$ ). The mean of these distributions gives the corresponding wave speeds, 1.07575 for  $k_0 = 1/\sqrt{2}$  and 2.77146 for  $k_0 = 0.1$ . For initial data  $k_0 = 1/\sqrt{2}$  with a wave speed of 1.07575 the variance of  $\lambda$  is smaller. In (c) we have plotted for the two different initial data sets the instantaneous wave speed  $\lambda(t)$  and the corresponding time averaged wave speeds  $\Lambda_{\min}(t)$  with  $t_0 = 0, t_1 = t$ . We see faster convergence of the wave speed for initial data  $k_0 = 1/\sqrt{2}$  and again the reduced variability in the instantaneous wave speed.

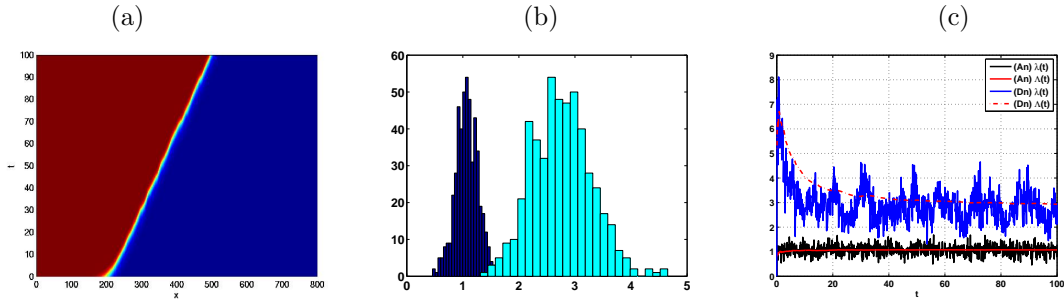


Figure 1: (a) Space-time plot of a single realization of the SPDE showing a travelling wave. In (b) distributions of the instantaneous wave speeds  $\lambda$  computed for the two different initial data sets. In (c) we plot  $\lambda(t)$  and the time averages  $\Lambda_{\min}(t)$  with  $t_0 = 0, t_1 = t$ .

Let us now compare to a single realization where the stochastic travelling wave is frozen and we solve the SPDAE (27) using the Heun method (28). Results on the wave speeds for the two initial data sets and two reference functions are reported in Table 4. We chose  $\Lambda_c$  and  $\Lambda_{\text{fit}c}$  to represent values computed from the level set approaches. The level sets no longer travel (on average) and hence have wave speeds with values close to zero. Note that the noise path is not the same as solving the SPDE for Table 3 and so we do not expect the values to be exactly the same, they are however close. The wave speed  $\Lambda_{\min}^{\text{fix}}$  estimated by the minimization is identical for the two different reference functions (solving the SPDAE we do not have the same interpolation errors as when solving the SPDE). However, the choice of reference function is an issue for the SPDE and we consider this further in Section 3.2.2.

In Figure 2 we have plotted in (a) the space-time plot of solution of the SPDAE. The front starts at  $x \approx 200$  and remains (on average) at that position throughout the computation illustrating that the wave does not travel (compare to Figure 1 (a)). In (b) for the two different initial data  $k_0 = 1/\sqrt{2}$  (with mean 1.08522) and  $k_0 = 0.1$  (with mean 2.74311) we have plotted the two distributions of the instantaneous wave speed  $\lambda$  used to compute the wave speed through the minimization (with  $\hat{k} = 1/\sqrt{2}$ ). Comparing with Figure 1 (b) we see similar distributions and greater variance with initial data with  $k_0 = 0.1$  than  $k_0 = 1/\sqrt{2}$  (as in Figure 1). In (c) we have plotted for the two different initial data sets the instantaneous wave speed  $\lambda(t)$  and the time averaged wave speed  $\Lambda_{\min}(t)$  with  $t_0 = 0$ . We see faster convergence of the wave speed  $\Lambda(t)$  for

$t_0 = 50, t_1 = 100$	$\Lambda_{\min}^{fix}$	$\Lambda_{\gamma}^{fix}$	$\Lambda_c$	$\Lambda_{fitc}$
$k_0 = 1/\sqrt{2}, \hat{k} = 1/\sqrt{2}$	1.08522	1.08828	2.421e-04	-2.131e-04
$k_0 = 1/\sqrt{2}, \hat{k} = 0.1$	1.08522	1.08828	2.421e-04	-2.131e-04
$k_0 = 0.1, \hat{k} = 0.1$	2.74311	2.76005	-5.703e-02	-6.404e-03
$k_0 = 0.1, \hat{k} = 1/\sqrt{2}$	2.74311	2.76005	-5.703e-02	-6.404e-03

Table 4: Wave speeds computed from solving a single realization of the SPDAE with noise intensity  $\mu = 0.1$  and correlation length  $\xi = 0.1$ .

	$\Lambda_{\min}$ or $\Lambda_{\min}^{fix}$	$\Lambda_{\gamma}$ or $\Lambda_{\gamma}^{fix}$	$\Lambda_c$	$\Lambda_{fitc}$
SPDE	$1.08588 \pm 0.19680$	$1.08388 \pm 2.73e-03$	$1.08381 \pm 2.81e-03$	$1.08390 \pm 2.68e-03$
SPDAE	$1.08951 \pm 0.19512$	$1.08790 \pm 2.39e-03$	$-4.0e-05 \pm 2.0e-5$	$3.0e-05 \pm 2.0e-5$

Table 5: Expected values of the wave speeds taken over 100 realizations solving the SPDE and the SPDAE. Initial data taken with  $k_0 = 1/\sqrt{2}$ , and reference function with  $\hat{k} = 1/\sqrt{2}$ .

$k_0 = 1/\sqrt{2}$  than for  $k_0 = 0.1$ .

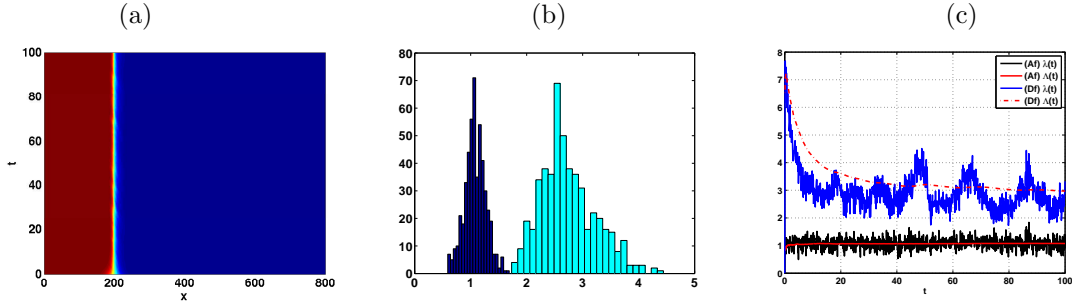


Figure 2: (a) Space-time plot of a single realization of the frozen SPDE showing a travelling wave. In (b) distributions of the instantaneous wave speeds  $\lambda$  computed for the two different initial data sets. In (c) we plot  $\lambda(t)$  and the time averages  $\Lambda_{\min}(t)$  with  $t_0 = 0, t_1 = t$ .

Rather than looking at a single realization more physically meaningful results are found from taking the expectation over many realizations. In Table 5 we examine wave speeds based on 100 realizations of both the SPDE and SPDAE. The different measures of the wave speed are in broad agreement. The larger uncertainty in  $\Lambda_{\min}$  and  $\Lambda_{\min}^{fix}$  originates in the large variance in the instantaneous wave speeds  $\lambda$  and is a drawback of the minimization approach.

We also compare the profiles from the SPDE to profiles obtained from the SPDAE. To avoid the spreading of the wave we need to align individual realizations of the SPDE. We chose as a common reference the level set  $c(100)$ . If we examine the final time profiles for the runs we find that the weak error,  $\|\mathbb{E}(u_{SPDAE}(100)) - \mathbb{E}(u_{SPDE}(100))\|_{L^2}^2$  for 10 realizations is  $\approx 0.0150$  and for 100 realizations  $\approx 0.0144$  and  $\approx 0.0117$  with 1000 realizations.

In Figure 3 we compare results for the SPDAE (a) and SPDE (b) for a range of different nonlinearity's  $\alpha \in \{-1, -0.5, -0.3, 0, 0.3, 0.45\}$  and noise intensities measured by  $\mu^2 \in [0, 1]$ . Initial data approximates a step function and the spatial correlation length of the noise  $\xi$  is that of the computational grid  $\Delta x$ . The results in (a), where  $\Delta x = \xi = 0.5$  where agree with those in [3, 2], reproduced in [16], where the authors obtain a front velocity taking an average over an “appropriate time window” of  $\int_L u(x, t) dt$  and compare to a small noise analysis. In (b) we took a smaller spatial step  $\Delta x = 0.1$  and have plotted the wave speed  $\Lambda_{\min}$  computed both from minimization and from the level set,  $\Lambda_c$  on which the error bars are based.

We observe that the effect of the two different approximations to spatially white noise is to increase the speed of the wave. Note that some realizations where the wave is frozen in Figure 3 (a) fail to exist due to numerical instability, see Section 3.2.1.

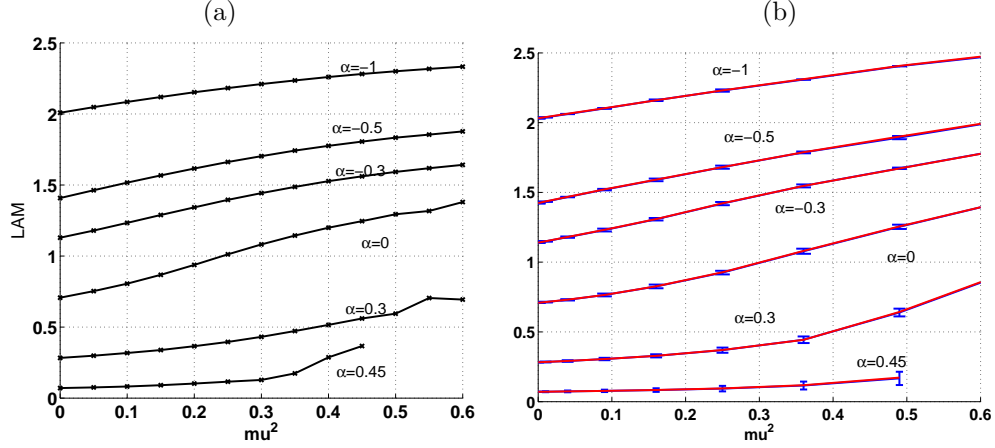


Figure 3: Wave speeds  $\Lambda_{\min}$  with increasing noise intensity for Stratonovich noise with correlation length equal to that of the grid. In (a) solving the SPDAE where the wave is frozen with  $\xi = 0.5 = \Delta x$  (b) the SPDE with  $\xi = 0.1 = \Delta x$ . Each line corresponds to a different nonlinearity with  $\alpha \in \{-1, -0.5, -0.3, 0, 0.3, 0.45\}$ .

### 3.2.1 Numerical instability

The numerical approximation of SDEs and SPDEs where the solution is constrained in phase space is an area under development. For the Nagumo equations (14) (or (15))  $u \in [0, 1]$ , another typical example is a positivity constraint where  $u > 0$ . Numerical instability can lead to non-physical solutions and potentially to unphysical unbounded growth of the numerical solution. A number of approaches have been proposed to simulations to enforce constraints on the numerics and a review of these types of methods for SDEs is contained in [22]. One method to avoid unbounded growth in numerics from nonphysical solutions the nonlinearity and noise can be adapted as in [25, 12, 11, 35].

We found that solving the SPDEs (14) (or (15)) such instability was not an issue. However, when freezing the wave and solving the SPDAE (27) did lead to non-physical solutions. In Figure 4 we have frozen the wave and show one realization at  $t = 34.7$  (a) with an instantaneous wave speed 10.98 and (b)  $t = 35.2$  with an instantaneous speed  $-10.60$ . The non-physical regions where  $u < 0$  and  $u > 1$  then grow in magnitude with further iterations.

Figure 1 and Figure 2 show the distribution of the instantaneous wave speed  $\lambda$  as computed for the SPDE and SPDAE respectively where the wave is frozen. The SPDAE system (27) includes the advection term  $\lambda v_x$ , where  $\lambda$  is a random variable with a particular distribution - which may lead to either large positive and/or negative values of  $\lambda$ . Numerically this is particularly true for large noise intensities or small correlation lengths of the noise. The result of this is a loss of numerical stability. Although we were able to control unbounded growth by modifying the equation solved close to the  $u = 0$  and  $u = 1$ , direct comparisons of wave speeds to SPDE calculations showed this can lead to a bias in the estimate, so we do not include such results here. Hence, in Figure 3 (a) results for the SPDAE equation are reported with the expectation taken over solutions that existed to the final time. A large number of initial realizations was taken so that the final expectation is over at least 1000 realizations. Although we observe the same results calculating the wave speed based on level set methods, in general not taking the results where there is numerical blow up may bias the statistics.

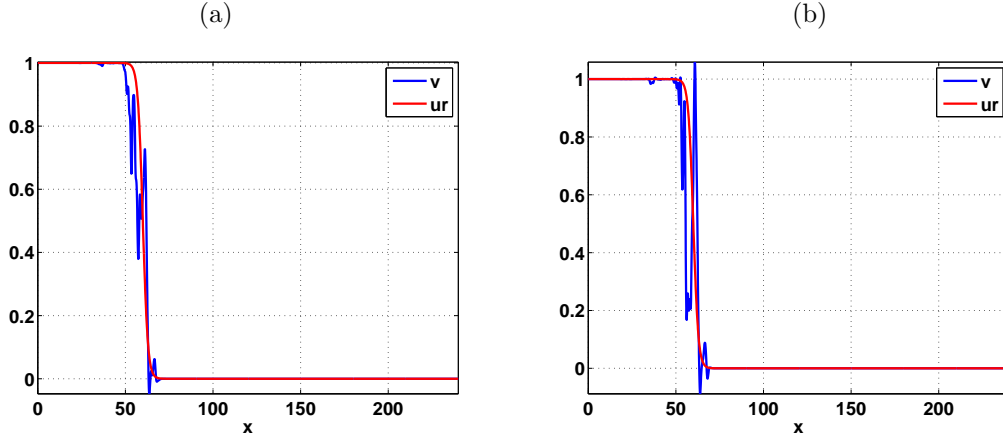


Figure 4: Plot of realization of a single realization of the noise illustrating instability (a) at  $t = 34.7$  and (b)  $t = 35.2$ , with corresponding instantaneous wave speeds of 10.98 and  $-10.60$ .

### 3.2.2 Choice of reference function $\hat{u}$ for the minimization

We commented early that natural choice for the reference function would be to take either a deterministic travelling wave or the initial data. However, the width of the reference function  $\hat{u}$  plays an important role in the computed wave speed for both the SPDE and SPDAE. If we take the reference function  $\hat{u}$  to be the Heaviside function then the minimization of the  $L^2$  norm fails. We observe numerically that narrow reference functions can also lead to numerical failure of the minimization and indeed there may be more than one minimal position.

To illustrate this we solve the SPDE with  $\alpha = 0.25$  and examine large noise intensity  $\mu = 1$  combined with a small correlation length of  $\xi = 0.5$ . In Figure 5 (a) with  $\hat{u} = u_k$ ,  $k = 1/\sqrt{2}$  we see that the width of the computed front is larger than the width of the reference function  $\hat{u}$  and in (b) is plotted the corresponding instantaneous wave speed  $\lambda(t)$  - with time average 0.6483 and variance of 6.4568. In (b) the reference function  $\hat{u} = u_{\hat{k}}$  has  $\hat{k} = 0.1$  and the width of the reference is larger than the solution. In (d) is plotted the corresponding instantaneous wave speed  $\lambda(t)$  - with time average 0.6091 and variance over time of 3.8006. In (a) the computation of the minimization fails at a later time ( $T \approx 55$ ) however in (b) computation was continued to  $T > 100$ . In (a) the minimization of the  $L^2$  norm is dominated by the random fluctuations in the front which is avoided with a template function with larger support. Provided the width of the reference function is comparable or larger than the width of the front the computations are robust although convergence rates of the wave speed can be much slower for poor choices of the reference function.

### 3.3 Effects of Stratonovich and Itô noise

Accurate numerical calculations are notoriously difficult in the deterministic case when the wave profile depends on the leading profile of the wave, see for example [13] for the Nagumo equation or [29] for the Fisher equation. We consider from now on initial data that converges to the minimum speed wave in the deterministic case and take initial data  $u_0 = u_k$  close to a step function with  $k = 50$ . We examine the effects on wave speed and support of the front from changing the noise intensity and correlation length for both Stratonovich and Itô noise.

First we examine the effects of Stratonovich noise on the travelling wave in the Nagumo equation. Figure 6 shows wave speed as noise intensity  $\mu$  increases for four different correlation lengths  $\xi = 0.1, 0.5, 1$  and 10. On each plot are plotted different nonlinearities  $\alpha = 0.3, 0.25, 0, -0.25, -0.3, -0.5, -1$ . Each point on the plot is an average over 100 realizations and wave speeds measured both from minimization  $\Lambda_{\min}$  and from the level set  $\Lambda_c$ . In Figure 6 we have

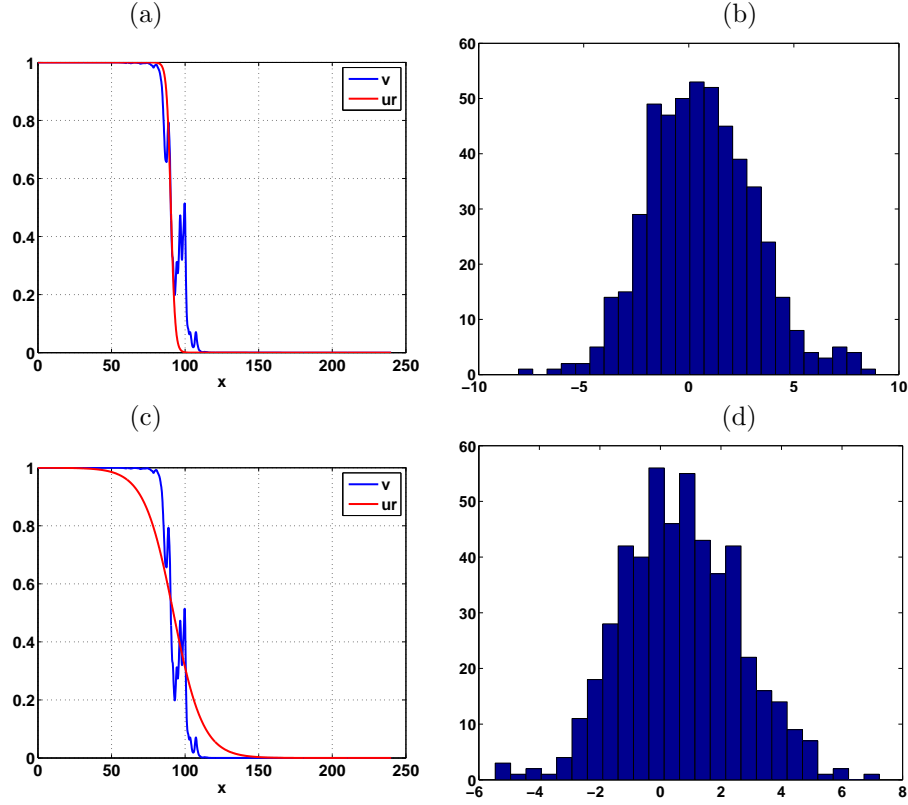


Figure 5: One realization of the solution with two different reference functions  $\hat{u} = u_k$  at time  $t = 50$  (a) and (c) and the corresponding different distributions of the instantaneous wave speeds  $\lambda(t)$  (b) and (d). In (a) and (b)  $\hat{k} = 1/\sqrt{2}$  and (c) and (d)  $\hat{k} = 0.1$ . Note the smaller variance in (d) with  $\hat{k} = 1/\sqrt{2}$ .

plotted the corresponding average widths. We see that increasing the noise intensity increases the wave speed, where as increasing the correlation length of the noise decreases the wave speed. The two effects essentially cancel each other in (d) and we see no overall effect on the noise intensity on the wave speed. We can also examine the form of the wave profile. In Figure 6 we have plotted the corresponding average widths of the wave as noise intensity  $\mu$  and correlation length  $\xi$  are changed. For large noise the width of the waves increase and this effect is again reduced as the correlation length is increased. For a spatial correlation length  $\xi = \Delta x = 0.1$  we have an approximation of white noise in space, for this case we see that for  $\alpha = 0.45$  and  $\alpha = 0.25$  the width of the wave increases and a larger computational domain is required.

For Itô noise the effect of the noise on wave speed and width of the waves is less pronounced, see Figure 8 for the wave speed and Figure 9 for the corresponding width of the waves. We see that for large noise, in contrast to the Stratonovich case, a slight drop in the wave speed for a correlation length  $\xi < 10$ . As we change the noise intensity we see (for most nonlinearities) a drop in the width of the wave – and so the front is steeper on average and the effect is more pronounced for shorter correlation lengths.

### 3.4 Computations using averaged quantities

In general computing wave profiles using averaged quantities leads to the wave being ‘polluted’ by the spread of the individual waves (see [16]).

In (32) we propose using an expected value of the instantaneous wave speeds for the SPDAE.

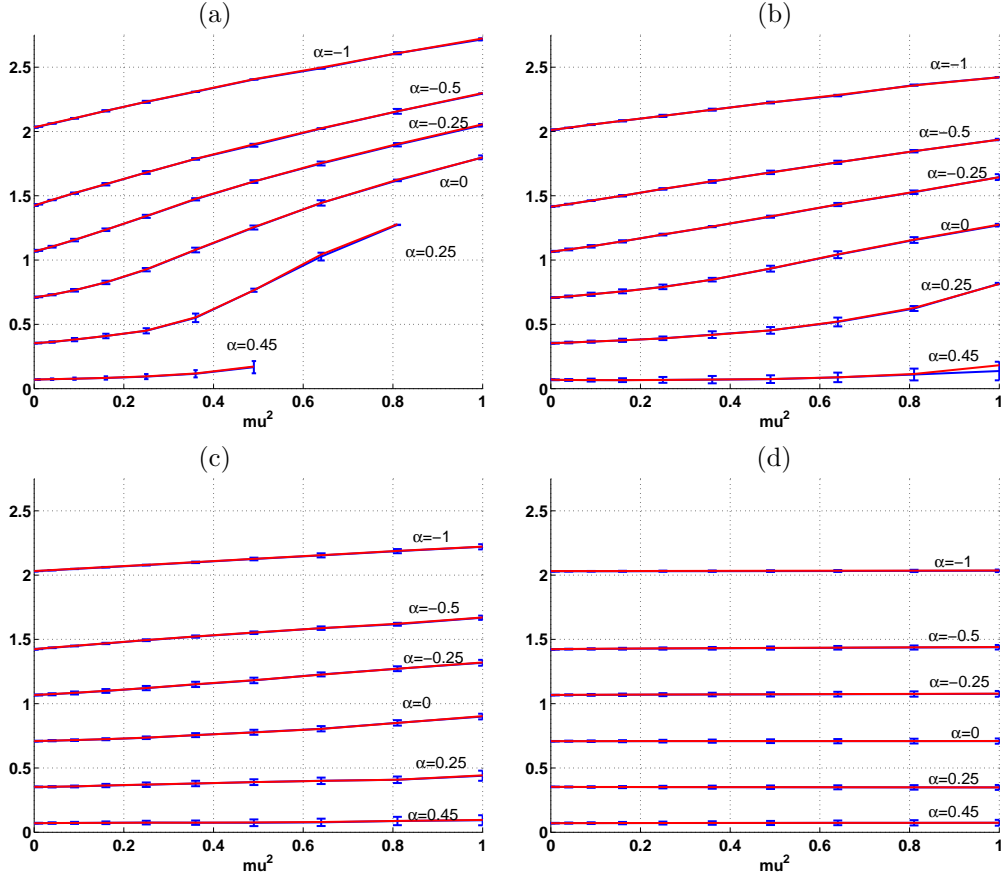


Figure 6: Wave speeds  $\Lambda_{\min}$  and  $\Lambda_c$  for increasing Stratonovich noise intensity and different spatial correlation lengths (a)  $\xi = 0.1$ , (b)  $\xi = 0.5$ , (c)  $\xi = 1$  and (d)  $\xi = 10$ . Increasing the noise intensity increases the expected wave speed where as increasing the correlation length decreases the expected wave speed.

We fix a spatial correlation of  $\xi = 0.5$ . For the SPDAE if we solve with  $\mu = 0.1$ ,  $\hat{u} = u_k$  with  $k = 0.1$  and  $u^0 = u_{k_0}$ ,  $k_0 = 1/\sqrt{2}$  and 100 realizations then we obtain an estimate of a wave speed of 1.086. This compares with  $\Lambda_{\min} = 1.086$  and  $\Lambda_c = 1.084$  from solving the SPDE (14). If we examine the computed mean solution front we do not observe spreading of the wave front (see Figure 10 (a)). We also note from (b) that the distribution of  $\lambda(t)$  has smaller variance than that from solving (27). For the SPDE we can implement a version (32) where we move the reference function using the expected values of the instantaneous wave speeds. In Figure 10 (c) we plot the distribution of  $\lambda$  for same parameters as in (b). The mean values agree although the distributions are different. In (d) we see that computed wave speeds using the average instantaneous speed and wave speeds  $\Lambda_c$  computed using the level set approach are the same over a range of nonlinearities. These are the same as those computed using the SPDE, compare to Figure 6 (b).

### 3.5 Additive noise

We briefly consider the case of additive noise in the SPDE for which, unless the noise has some special properties, a solution will in general cease to exist at some finite time.

We now change the parameter  $\alpha$  in the nonlinearity to  $\alpha = 0.1$  and illustrate how the SPDAE approach deals with nucleation and extinction of waves. In Figure 12 we have plotted in (a) a single realization of the SPDE (so not frozen) showing nucleation and subsequent extinction ( $t \approx 98$ ) of a

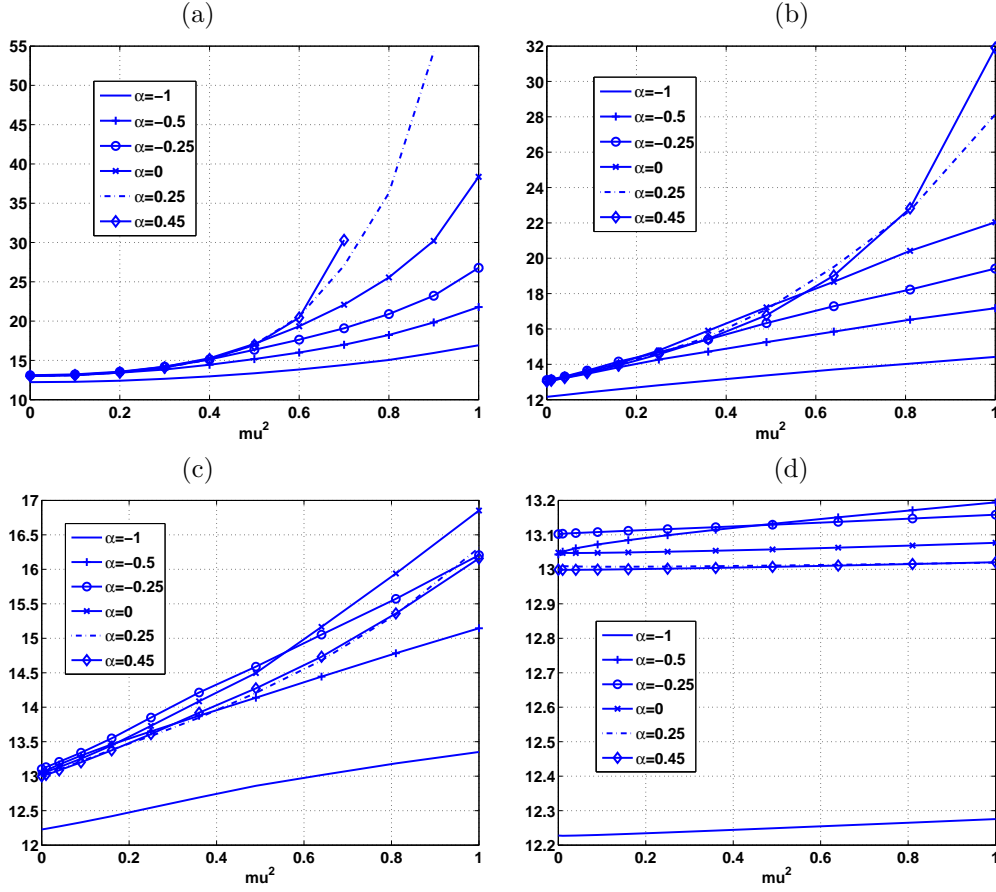


Figure 7: Expected width of the wave for increasing Stratonovich noise intensity and different spatial correlation lengths (a)  $\xi = 0.1$ , (b)  $\xi = 0.5$ , (c)  $\xi = 1$ , and (d)  $\xi = 10$ . As the noise intensity is increased the expected width of the wave front increases where as for fixed intensity increasing the correlation length reduces the expected width.

travelling wave. In (b) is plotted a single realization from computing using the SPDAE approach. We see the wave is fixed in the domain and at  $t \approx 50$  a wave is nucleated at  $x \approx 100$  by the additive noise. The computations are based on the original wave which remains fixed until it interacts with the nucleated wave and is annihilated at  $t \approx 94$  when the computations stop when the wave cease to exist. In (c) and in (d) we have plotted mean profiles for the SPDE and the frozen SPDAE systems. In each case we see a well defined front from the averaging and individual nucleations and annihilations are no longer distinguishable (although in (d) a large solution pollutes the data at  $t \approx 130$ ).

## 4 Discussion

We have examined level set based methods and minimization to a reference function methods to calculate the wave speed of a stochastic travelling wave. Our numerical results illustrate these give comparable results. Numerically we saw that for reference functions with support much smaller than the support of the travelling wave that the minimization may fail. Using the minimization technique for the SPDE (when it is not frozen) is more computationally expensive than the level set based methods as it requires interpolation at each time step.

The algorithm described for freezing the wave and solving the SPDAE has several numerical



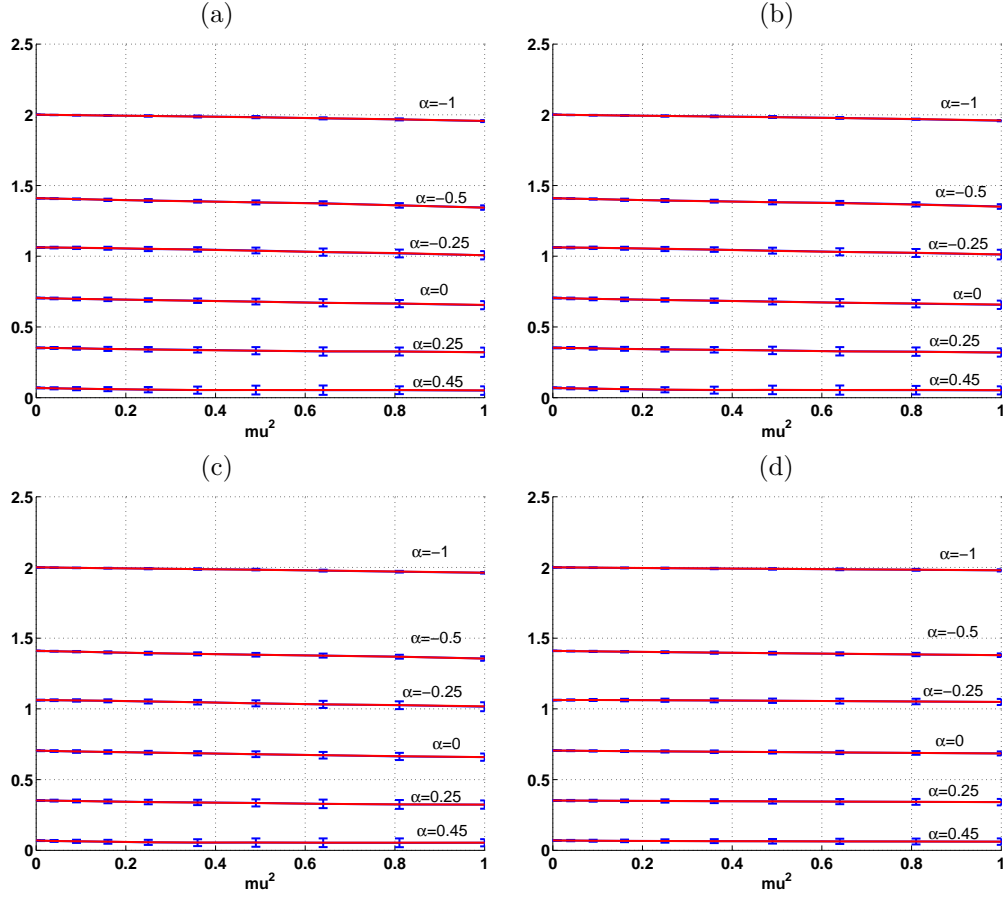


Figure 8: Expected wave speeds  $\Lambda_{\min}$  and  $\Lambda_c$  for increasing Itô noise intensity and different spatial correlation lengths (a)  $\xi = 0.1$ , (b)  $\xi = 0.5$ , (c)  $\xi = 1$  and (d)  $\xi = 10$ . As noise intensity is increased we see a slight drop in wave speed and little effect from the changing correlation length.

advantages over simply solving the SPDE if the numerical instability issues could be overcome. The frozen wave does not require a large computational domain for long time simulations and the generation of the noise path is not so computationally expensive. The cost of the minimization when the wave is fixed is minimal as we simply need to compute two inner-products. However the advection term is nontrivial - and the loss of numerical stability is a real issue where some realizations fail to exist as ignoring results where there is numerical blow up may bias the statistics.

Our investigation of the Nagumo equation has revealed interesting and new computational observations that we have not seen reported in the literature. Although it was known that for Stratonovich noise increasing noise intensity increases wave speed we have also seen it increases the support of the wave. In addition increasing the spatial correlation decreases the wave speed and decreases the support of the wave. The reverse is observed for Itô noise: the noise intensity seems to decrease the wave speed and correlation length has little influence on the speed decreases the support of the wave.

For additive noise in the Nagumo equation we see that the wave speed is increased with the noise intensity like in the multiplicative case - this is probably because of the small perturbations ahead of the front that make the wave faster.

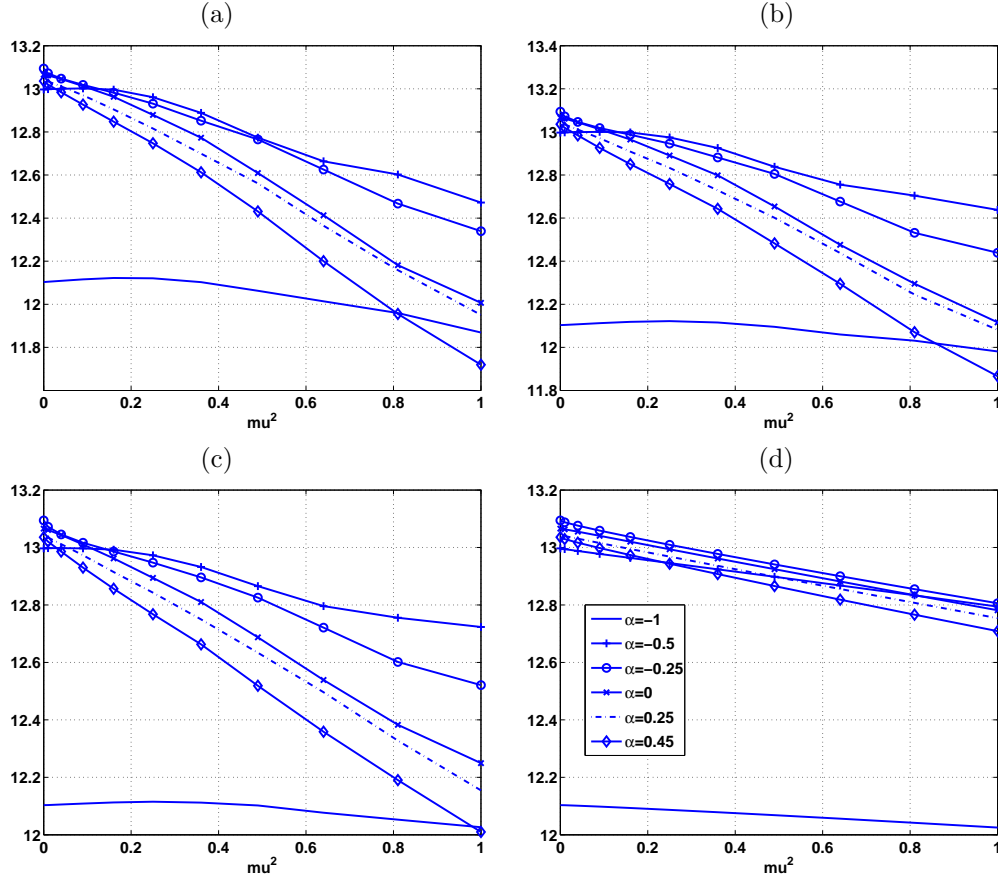


Figure 9: Expected width of waves for increasing Itô noise intensity and different spatial correlation lengths (a)  $\xi = 0.1$ , (b)  $\xi = 0.5$ , (c)  $\xi = 1$  and (d)  $\xi = 10$ . Increasing noise intensity narrows the width of the wave and this effect is mitigated by increasing the correlation length. Legend for all four plots is given in (d).

## References

- [1] H. AIRAULT, *Équations asymptotiques pour des cas spéciaux de l'équation de Nagumo*, C. R. Acad. Sci. Paris Sér. I Math., 301 (1985), pp. 295–298.
- [2] J. ARMERO, J. CASADEMUNT, L. RAMÍREZ-PISCINA, AND J. M. SANCHO, *Ballistic and diffusive corrections to front propagation in the presence of multiplicative noise*, Phys. Rev. E, 58 (1998), pp. 5494–5500.
- [3] J. ARMERO, J. M. SANCHO, J. CASADEMUNT, A. M. LACASTA, L. RAMÍREZ-PISCINA, AND F. SAGUÉS, *External fluctuations in front propagation*, Phys. Rev. Lett., 76 (1996), pp. 3045–3048.
- [4] U. M. ASCHER AND L. R. PETZOLD, *Computer methods for ordinary differential equations and differential-algebraic equations*, Society for Industrial and Applied Mathematics (SIAM), Philadelphia, PA, 1998.
- [5] W.-J. BEYN, S. SELLE, AND V. THÜMLER, *Freezing multipulses and multifronts*, Tech. Rep. 2, 2008.

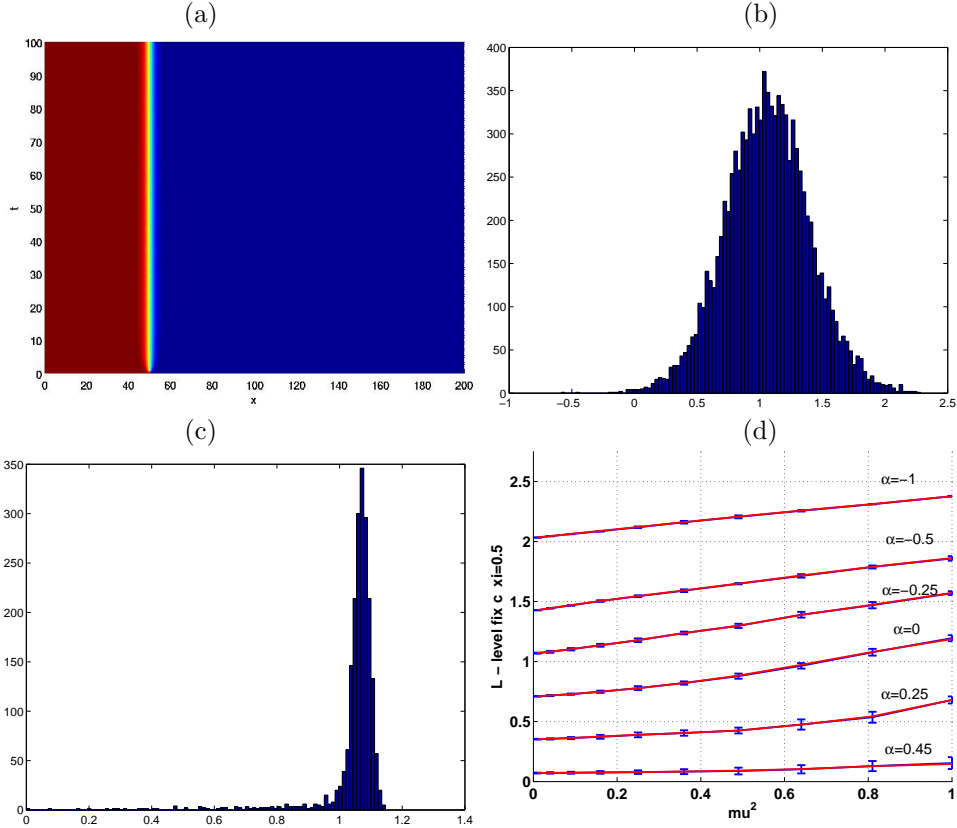


Figure 10: (a) Mean solution of SPDAE (32). Note that we do not observe that the wave front has been spread taking the mean instantaneous speed. In (b) is plotted the distribution of  $\lambda$  used to freeze the wave in (a). In (c) we plot the distribution from solving the SPDE using an average wave speed for the minimization and for the SPDE and in (d) we compare wave speeds over a range on nonlinearities and noise intensities for  $\xi = 0.5$ .

- [6] W.-J. BEYN AND V. THÜMLER, *Freezing solutions of equivariant evolution equations*, SIAM Journal on Applied Dynamical Systems, 3 (2004), pp. 85–116.
- [7] ———, *Numerical Continuation Methods for Dynamical Systems*, Series in Complexity, Springer, 2007, ch. Phase conditions, Symmetries, and PDE Continuation, pp. 301–330.
- [8] S. BRASSESCO, A. DE MASI, AND E. PRESUTTI, *Brownian fluctuations of the interface in the  $d = 1$  Ginzburg–Landau equation with noise.*, Annales de L’I.H.P. Section B., 31 (1995), pp. 81–118.
- [9] Z. X. CHEN AND B. Y. GUO, *Analytic solutions of the Nagumo equation*, IMA J. Appl. Math., 48 (1992), pp. 107–115.
- [10] G. DA PRATO AND J. ZABCZYK, *Stochastic Equations in Infinite Dimensions*, vol. 44 of Encyclopedia of Mathematics and its Applications, Cambridge University Press, Cambridge, 1992.
- [11] C. DOERING, K. SARGSYAN, AND P. SMEREKA, *A numerical method for some stochastic differential equations with multiplicative noise*, Physics Letters A, 344 (2005), pp. 149–155. doi:10.1016/j.physleta.2005.06.045.

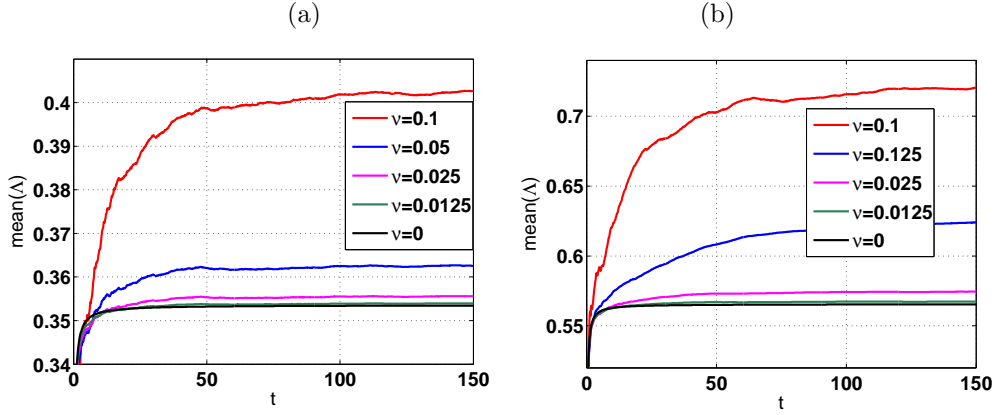


Figure 11: Influence of additive white noise on the wave speed  $\Lambda_{\min}$  for (a)  $\alpha = 0.25$  and (b)  $\alpha = 0.1$ . In both cases there is a clear increase in the wave speed from the deterministic case ( $\nu = 0$ ) as the noise intensity is increased, with the final wave speeds in order of the indicated noise intensities.

- [12] C. R. DOERING, C. MUELLER, AND P. SMEREKA, *Interacting particles, the stochastic Fisher-Kolmogorov-Petrovsky-Piscounov equation, and duality*, Phys. A, 325 (2003), pp. 243–259. Stochastic systems: from randomness to complexity (Erice, 2002).
- [13] C. ELMER AND E. S. VAN VLECK, *Dynamics of monotone travelling fronts for discretizations of nagumo pdes*, Nonlinearity, 18 (2005), pp. 1605–1628. doi:10.1088/0951-7715/18/4/010.
- [14] T. FUNAKI, *The scaling limit for a stochastic pde and the separation of phases*, Probability Theory and Related Fields, 102 (1995), pp. 221–288. DOI: 10.1007/BF01213390.
- [15] J. GARCÍA-OJALVO, J. M. R. PARRONDO, J. M. SANCHO, AND C. VAN DEN BROECK, *Reentrant transition induced by multiplicative noise in the time-dependent ginzburg-landau model*, Phys. Rev. E, 54 (1996), pp. 6918–6921.
- [16] J. GARCIA-OJALVO AND J. M. SANCHO, *Noise in Spatially Extended Systems*, Institute for nonlinear Science, Springer-Verlag, New York, 1999. ISBN 0-387-98855-6.
- [17] M. HAIRER AND J. VOSS, *Approximations to the stochastic burgers equation*, arXiv:1005.4438v1, (2010).
- [18] S. A. J. NAGUMO AND S. YOSHIKAWA, *An active pulse transmission line simulating nerve axon.*, in Proceedings of the IRE, vol. 50, 1962, pp. 2061–2070.
- [19] A. JENTZEN AND M. RÖCKNER, *Regularity analysis for stochastic partial differential equations with nonlinear multiplicative trace class noise*, arXiv:1005.4095v1, (2010).
- [20] P. E. KLOEDEN AND E. PLATEN, *Numerical solution of stochastic differential equations*, vol. 23 of Applications of mathematics, Springer-Verlag, 1992.
- [21] G. J. LORD AND J. ROUGEMONT, *A numerical scheme for stochastic PDEs with Gevrey regularity*, IMA J Num. Anal., 24 (2004), pp. 587–604.
- [22] R. LORD, R. KOEKKOEK, AND D. DIJK, *A comparison of biased simulation schemes for stochastic volatility models.*, tech. rep., Tinbergen Institute, 2006.
- [23] A. S. MIKHAILOV, L. SCHIMANSKY-GEIER, AND W. EBELING, *Stochastic motion of the propagating front in bistable media*, Physics Letters A, 96 (1983), pp. 453–456.

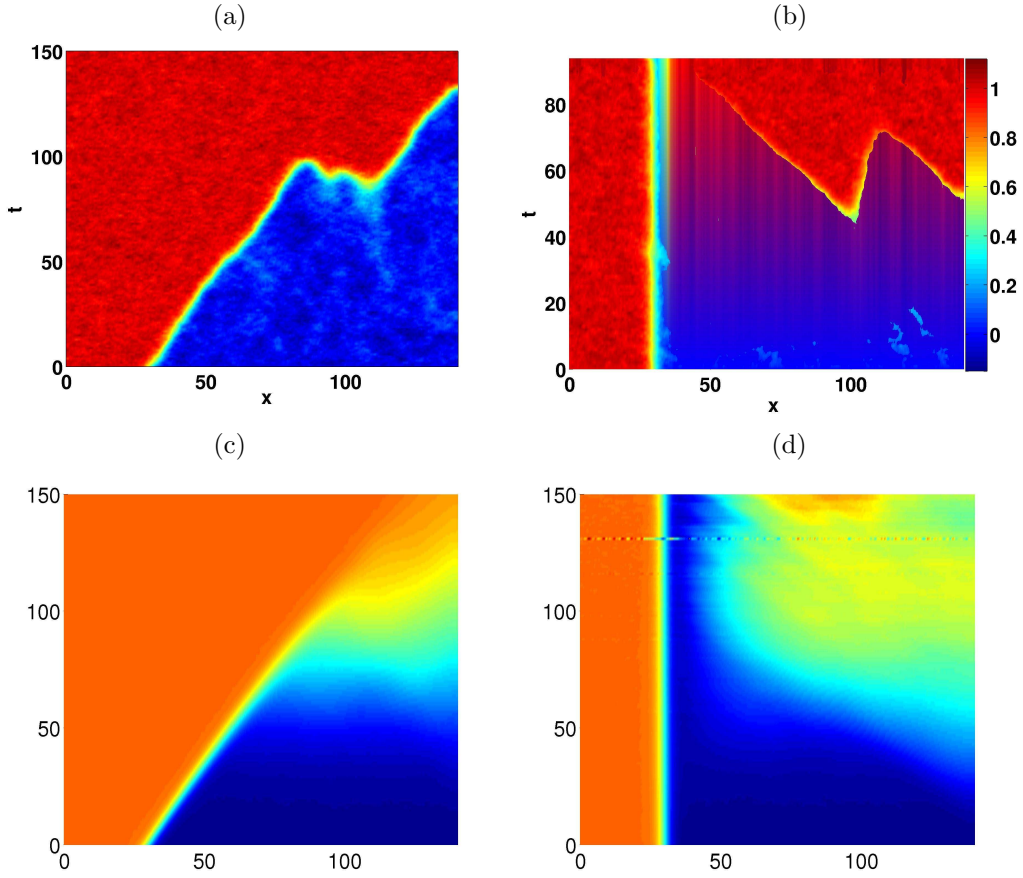


Figure 12: Nucleation of travelling waves and annihilation for the Nagumo equation with  $\alpha = 0.1$ . In (a) the space-time plot shows computations of the SPDE (no freezing) and in (b) the SPDAE where the wave is frozen. In (c) and (d) are plotted means over realizations for the frozen and travelling cases.

- [24] E. MORO, *Numerical schemes for continuum models of reaction–diffusion systems subject to internal noise*, Physical Review E., (2004).
- [25] E. MORO AND H. SCHURZ, *Boundary preserving semianalytic numerical algorithms for stochastic differential equations*, SIAM J. Scientific Computing, 29 (2007), pp. 1525–1549.
- [26] C. MUELLER AND R. SOWERS, *Travelling waves for the KPP equation with noise*, in Stochastic analysis (Ithaca, NY, 1993), vol. 57 of Proc. Sympos. Pure Math., Amer. Math. Soc., Providence, RI, 1995, pp. 603–609.
- [27] D. PANJA, *Effects of fluctuations on propagating fronts*, Physics Reports., 393 (2004), pp. 87–174. doi:10.1016/j.physrep.2003.12.001.
- [28] C. PRÉVÔT AND M. RÖCKNER, *A Concise Course on Stochastic Partial Differential Equations*, no. 1905 in Lecture Notes in Mathematics, Springer, 2007.
- [29] Y. QIU AND D. M. SLOAN, *Numerical solution of Fisher’s equation using a moving mesh method*, J. Comput. Phys., 146 (1998), pp. 726–746.

- [30] W. RÖMISCH AND R. WINKLER, *Stochastic DAEs in circuit simulation*, in Modeling, simulation, and optimization of integrated circuits (Oberwolfach, 2001), vol. 146 of Internat. Ser. Numer. Math., Birkhäuser, Basel, 2003, pp. 303–318.
- [31] J. ROUGEMONT, *Space-time invariant measures, entropy, and dimension for stochastic Ginzburg-Landau equations*, Comm. Math. Phys., 225 (2002), pp. 423–448.
- [32] C. W. ROWLEY, I. G. KEVREKIDIS, J. E. MARSDEN, AND K. LUST, *Reduction and reconstruction for self-similar dynamical systems*, Nonlinearity, 16 (2003), pp. 1257–1275.
- [33] O. SCHEIN AND G. DENK, *Numerical solution of stochastic differential-algebraic equations with applications to transient noise simulation of microelectronic circuit*, Journal of Computational and Applied Mathematics, 100 (1998), pp. 77–92.
- [34] T. SHARDLOW, *Stochastic perturbations of the Allen–Cahn equation*, Electronic J. of Differential Equations, (2000), pp. 1–19. ISSN:1072-6691.
- [35] T. SHARDLOW, *Numerical simulation of stochastic PDEs for excitable media*, J. Comput. Appl. Math., 175 (2005), pp. 429–446.
- [36] T. SHIGA, *Two contrasting properties of solutions for one-dimensional stochastic partial differential equations*, Canad. J. Math., 46 (1994), pp. 415–437.
- [37] V. THÜMMLER, *Numerical Analysis of the method of freezing traveling waves*, PhD thesis, Bielefeld University, 2005.
- [38] ———, *Asymptotic stability of discretized and frozen relative equilibria*, Tech. Rep. 2, 2008.
- [39] R. TRIBE, *A travelling wave solution to the Kolmogorov equation with noise*, Stochastics, 56 (1996), pp. 317–340.
- [40] J. WALSH, *An introduction to stochastic partial differential equations.*, in Ecole d’ete de probabilités de Saint-Flour XIV, D. Williams, ed., vol. 1180 of Lect. Notes Math., Springer, 1986, pp. 265–437.
- [41] R. WINKLER, *Stochastic differential algebraic equations of index 1 and applications in circuit simulation*, J. Comput. Appl. Math., 157 (2003), pp. 477–505.
- [42] ———, *Stochastic differential algebraic equations in transient noise analysis*, in Proceedings of ‘Scientific Computing in Electrical Engineering’, Mathematics in Industry, Sept 2004.
- [43] B. XIE, *The stochastic parabolic partial differential equation with non-Lipschitz coefficients on the unbounded domain*, J. of Mathematical Analysis and Applications, 339 (2008), pp. 705–718.